Magnetostructural transition in $Gd_5Si_{0.5}Ge_{3.5}$: Magnetic and x-ray powder diffraction measurements, and theoretical calculations

Ya. Mudryk,[1] D. Paudyal,[1] V. K. Pecharsky,[1,2,*] and K. A. Gschneidner, Jr.[1,2]
[1]*Ames Laboratory, Iowa Sate University, Ames, Iowa 50011-3020, USA*
[2]*Department of Materials Science and Engineering, Iowa State University, Ames, Iowa 50011-2300, USA*
(Received 14 May 2007; revised manuscript received 27 July 2007; published 9 January 2008)

Magnetostructural transition, which occurs at 77 K (89 K) in the heat-treated (as cast) $Gd_5Si_{0.5}Ge_{3.5}$, has been examined both experimentally, by magnetic and x-ray powder diffraction measurements, and theoretically, by *ab initio* calculations. Similar to that observed in a related $Gd_5Si_{0.4}Ge_{3.6}$ alloy, this first-order phase transformation from a high-temperature Sm_5Ge_4-type [O(II)] phase to a low-temperature Gd_5Si_4-type [O(I)] phase is accompanied by an antiferromagnetic to ferromagnetic transition. The *H-T* phase diagram, which includes both structural and magnetic features, has been constructed. The total energy as a function of unit-cell volume calculated from first principles confirms the experimentally observed first-order nature of the magnetostructural transformation. Experimental results supported by theoretical calculations indicate that Si promotes the O(II)-$Gd_5Si_{0.5}Ge_{3.5}$ to O(I)-$Gd_5Si_{0.5}Ge_{3.5}$ transformation by exerting chemical pressure.

DOI: 10.1103/PhysRevB.77.024408 PACS number(s): 81.30.Hd, 61.50.Ks, 71.20.−b, 75.30.Kz

INTRODUCTION

Understanding the interplay between crystal and magnetic structures is an important challenge in materials physics. The $Gd_5Si_xGe_{4-x}$ system exhibits an interesting example of this phenomenology due to the peculiar nature of its crystal structure. The discovery of the giant magnetocaloric effect at 270 K in this system at $x=2$ drew much attention.[1] Soon after, the colossal magnetostriction and giant magnetoresistance were observed in $Gd_5Si_{1.8}Ge_{2.2}$.[2,3] Within a few years, additional reports of other exotic behaviors in these exceptional materials appeared in the literature. These include an unusual Hall effect,[4] spontaneous generation of voltage,[5] training effects,[6–10] unusual dynamical and thermal effects,[11–16] acoustic emissions,[17] and an unconventional frozen magnetic glasslike state.[18] In particular, for $Gd_5Si_2Ge_2$, most of the interesting physics was associated with a structural transformation between the monoclinic $Gd_5Si_2Ge_2$-type and the orthorhombic Gd_5Si_4-type structures coupled with the magnetic ordering-disordering transition between the paramagnetic (PM) and ferromagnetic (FM) states.[19]

The magnetostructural transition (MST) temperature in $Gd_5Si_xGe_{4-x}$ alloys with $x \leqslant 2.1$ is strongly dependent on the chemical composition of an alloy, and it increases with increasing Si content (x).[20–22] When $0 \leqslant x \leqslant 1$, the paramagnetic state first transforms to an antiferromagnetic (AFM) one, which, upon further cooling, evolves into the FM state. However, for alloys with $1 < x \leqslant 2.1$, long range ferromagnetic order forms directly from the paramagnetic phase. Morellon *et al.*[23] showed that the AFM↔FM transition in $Gd_5Si_{0.4}Ge_{3.6}$ is coupled with a structural transformation between the Sm_5Ge_4-type [O(II)] structure and Gd_5Si_4-type [O(I)] structure. A large magnetostriction observed in this material during MST is due to pronounced displacements of the atomic layers along the *a* axis.[23–25] This martensitic-like transformation is characterized by an abrupt change of lattice parameters and atomic positions, but the symmetry remains unaffected (space group is *Pnma* for both phases).[23,25]

Crystallographically, the MST in $Gd_5Si_{0.4}Ge_{3.6}$ is identical to that of Gd_5Ge_4, where the O(II)↔O(I) transformation is only observed in the presence of a magnetic field or under pressure.[25–27] In Gd_5Ge_4, the Sm_5Ge_4-type structure is stable at low temperatures in low magnetic fields, whereas in fields higher than $\mu_0 H = 1.6$ T, it is replaced with the Gd_5Si_4-type phase. Due to addition of Si, a magnetic field is no longer required for the O(II) AFM↔O(I) FM transition to take place, thus indicating that Si has a strong effect on the ground state of $Gd_5Si_xGe_{4-x}$. In addition to the colossal magnetostriction and giant magnetoresistance, an interesting thermoelectric behavior and unusual changes in the electrical resistivity near the first-order phase transition were observed in $Gd_5Si_{0.4}Ge_{3.6}$.[6,8,23,28,29] The mechanism of how the Si atoms influence the magnetism and lattice behavior of the $Gd_5Si_xGe_{4-x}$ alloys involves the effects of chemical pressure when the smaller Si atom substitutes for the larger Ge atom in the crystal lattice.[30]

In the past, only $Gd_5Si_2Ge_2$ was studied in detail using first-principles computations, resulting in the calculation of the electronic structure and magnetic, magneto-optical, *x*-ray magnetic circular dichroism, and giant magnetoresistance properties.[31–36] Another recent study coupled electronic structure calculations of $Gd_5Si_2Ge_2$ with the mean field theory, leading to a reasonable agreement of both the theoretically predicted magnetostructural transition temperature and the magnetocaloric effect with experimentally observed values, thus paving the way toward studying coupled magnetic and structural transitions from first principles in other $Gd_5Si_xGe_{4-x}$ compounds.[37] More recently, some basic issues related to the electronic, magnetic, and structural properties of Gd_5Ge_4 were addressed from first-principles electronic structure theory in order to lay a foundation toward understanding the origin of ferromagnetism in this compound.[38]

Here, we determine the nature of the O(I)↔O(II) transition in $Gd_5Si_xGe_{4-x}$ ($0 < x \leqslant 1$) through systematic magnetic, crystallographic, and electronic structure studies of $Gd_5Si_{0.5}Ge_{3.5}$ using a much higher purity Gd starting material than has been used in some earlier studies of samples having a similar composition. For this purpose, high-resolution x-ray powder diffraction data as a function of tem-

perature and magnetic field were combined with a detailed study of the magnetic properties and theoretical band structure calculations.

EXPERIMENTAL PROCEDURE

A 20 g button of $Gd_5Si_{0.5}Ge_{3.5}$ alloy was prepared by arc melting of the high purity elements under purified argon atmosphere. The Gd with purity better than 99.9 wt % (99.8 at. %) was prepared by the Materials Preparation Center,[39] while Si and Ge with a purity better than 99.999 wt % were obtained from commercial vendors. The major impurities (in ppm at.) in Gd were F (910), O (658), C (187), N (67), and Y (35), while commercial grade Gd used to prepare the $Gd_5Si_{0.4}Ge_{3.6}$ alloy in Refs. 6, 8, 23, 28, and 29 is 95–93 at. % pure with the interstitial impurities—H, C, N, and O—typically between 3000 and 15 000 ppm at. each. One part of the prepared alloy was sealed in a Ta crucible under He atmosphere and annealed at 1300 °C for 1 h. Another part was investigated in the as cast condition. The phase purity was analyzed at room temperature by x-ray powder diffraction, and both the as cast and heat-treated samples were found to be single phase materials within the sensitivity of this technique.

The magnetic properties were measured using a Quantum Design MPMS-XL7 superconducting quantum interference device (SQUID) magnetometer. Magnetization measurements were carried out as a function of temperature in constant dc magnetic fields of 0.05, 2, and 4 T over the range of temperatures from 2 to 300 K, and isothermally as a function of applied dc magnetic field at 2 K, 8 K, and at several temperatures near the MST over the range of magnetic fields from 0 to 7 T. In order to directly compare the x-ray powder diffraction results with the magnetic properties, the measurements of dc magnetization were also performed using a sample extracted from a powder specimen, which was employed in the x-ray experiment. All measurements were performed after cooling a sample in zero magnetic field before application of the magnetic field.

The x-ray powder diffraction measurements were carried out on a Rigaku TTRAX rotating anode powder diffractometer employing Mo $K\alpha$ radiation. The diffractometer was equipped with a continuous flow ^{4}He cryostat controlling the temperature of a sample, and a split-coil superconducting magnet creating a homogeneous dc magnetic field around the specimen.[26] The fine powders for low-temperature x-ray diffraction were prepared as described elsewhere.[26,40] The scattered intensity was recorded as a function of Bragg angle (2θ) using a scintillation detector with a step of 0.01° 2θ in step scan mode, with the intensity measured for 2 s at each point. The maximum Bragg peak intensity to lowest background intensity ratio was close to 100, with the strongest Bragg peaks registering nearly 7000 counts at their peak values. The range of measured Bragg angles was from 9° to 52° of 2θ, which is equivalent to about 19.5°–117° 2θ range when using Cu $K\alpha$ radiation ($\sin\theta_{\max}/\lambda \cong 0.553$).

RIETICA LHPM[41] software was employed for the full-profile Rietveld refinement of every recorded pattern. The coordinates of individual atoms were refined if the concentration of the corresponding phase was 20 mol % or more. The isotropic displacement parameters of all atoms in each phase were assumed to be the same, in effect, employing the overall isotropic displacement approximation. The profile residuals R_p were from ~0.08 to ~0.10, and the derived Bragg residuals R_B were from ~0.04 to ~0.06. The quantitative phase analysis was performed taking into account assumptions discussed in Ref. 40, and errors in phase content determination were ~1 mol %, following least squares standard deviations of the corresponding scale factors.

ELECTRONIC STRUCTURE METHOD

The local spin density approximation with an on-site Coulomb parameter (LSDA+U) correlated band approach[42,43] was employed to investigate the electronic and magnetic properties of the $Gd_5Si_{0.5}Ge_{3.5}$ system as a function of crystal structure. The advantage of this approach over LSDA and details of its implementation have been discussed in a recent publication[37] (see also references therein). The calculations have been performed using the scalar relativistic version (which includes the mass velocity and Darwin correction terms) of the LSDA+U method implemented in the tight binding linear muffin-tin orbital[44] scheme with U=6.7 eV and exchange interaction parameter J=0.7 eV.[42] Here, the parametrization of Langreth and co-workers[45–47] for exchange correlation functional has been employed because it resulted in estimates that were closest to experimental values for the transition temperatures in a related $Gd_5Si_2Ge_2$ system[37] as compared to the von Barth–Hedin[48] local exchange correlation or the Perdew-Wang[49,50] nonlocal exchange correlation, which, respectively, underestimate and overestimate transition temperatures. A total of 125 special k points in the irreducible part of the Brillouin zone were used for k space integrations.

The experimentally determined occupations (Table I) show that in $Gd_5Si_{0.5}Ge_{3.5}$ the interslab Ge3 positions are fully occupied by Ge atoms. The intraslab T1 and T2 positions are occupied randomly by 76% Ge and 24% Si. For theoretical calculations, Ge atoms were placed in all sites as a first model. In a second model, T1 and T2 positions were filled with Si. Final outputs (e.g., total energy and magnetic moments) were averages of the outputs of these two models weighed according to the experimentally determined occupations of the T1 and T2 positions by Ge and Si.

EXPERIMENTAL RESULTS AND DISCUSSION

Magnetic properties

The magnetization of the heat-treated $Gd_5Si_{0.5}Ge_{3.5}$ sample, measured as function of temperature in applied dc magnetic field of $\mu_0 H$=0.05 T, reveals two anomalies: the paramagnetic to antiferromagnetic transition at T_N=130 K, and the antiferromagnetic to ferromagnetic transition at T_C =77 K. The transition at T_C remains extremely sharp even in $\mu_0 H$=4 T field, shifting to higher temperatures with increasing field [T_C=94 K at 4 T, Fig. 1(a)]. Thermal hysteresis between the zero-field cooled heating and field cooling branches is about 1 K, which is much narrower compared to

TABLE I. Crystallographic data of the two $Gd_5Si_{0.5}Ge_{3.5}$ polymorphs at 8 and 100 K. The space group is *Pnma* in each case. The refined composition is $Gd_5Si_{0.48(6)}Ge_{3.52(6)}$. The data are for the heat-treated sample.

	$T=8$ K, Gd_5Si_4-type [O(I)][a]			$T=100$ K, Sm_5Ge_4-type [O(II)][b]		
Atom	x/a	y/b	z/c	x/a	y/b	z/c
Gd1	0.3482(5)	0.25	0.0087(4)	0.2935(4)	0.25	0.0023(4)
Gd2	0.0213(3)	0.0967(1)	0.1823(3)	−0.0250(2)	0.1003(1)	0.1795(3)
Gd3	0.3236(3)	0.8779(1)	0.1757(3)	0.3796(3)	0.8831(1)	0.1650(3)
T1[c]	0.2303(9)	0.25	0.3600(10)	0.1751(8)	0.25	0.3628(10)
T2[d]	0.9771(10)	0.25	0.8964(9)	0.9148(9)	0.25	0.8937(10)
Ge3	0.1643(7)	0.9605(3)	0.4811(6)	0.2215(6)	0.9548(2)	0.4714(6)

[a] $a=7.5311(3)$ Å, $b=14.7853(6)$ Å, and $c=7.7961(3)$ Å.
[b] $a=7.6709(3)$ Å, $b=14.7789(6)$ Å, and $c=7.7554(3)$ Å.
[c] T1=0.74(3)Ge+0.26(3)Si, constrained to be fully occupied.
[d] T2=0.78(3)Ge+0.22(3)Si, constrained to be fully occupied.

5–10 K observed in some other $Gd_5Si_xGe_{4-x}$ alloys.[2,51] The Curie temperature increases with applied magnetic field with $dT_C/dH=4.3$ K/T, which is slightly higher than 3.7 K/T reported for $Gd_5Si_{0.4}Ge_{3.6}$.[23] Similar to Gd_5Ge_4,[24] the Néel temperature shifts to lower temperatures as magnetic field increases with $dT_N/dH \cong -1$ K/T. The Curie-Weiss fit of the $\mu_0 H=4$ T data for 200 K$<T<$300 K (there is a positive deviation from linearity below 200 K) gives an effective magnetic moment $p_{\text{eff}}=8.01\mu_B$/Gd atom, which is close to the theoretical value, $g_J[J(J+1)]^{1/2}$ ($7.94\mu_B$), for a free Gd^{3+} ion. The Weiss temperature, $\theta_p=98$ K, is consistent with the ferromagnetic ground state of $Gd_5Si_{0.5}Ge_{3.5}$ and $T_C=77$ K.

Isothermal $M(H)$ measurements confirm the first-order nature of the AFM-FM transition [Fig. 1(b)]. The magnetization curves collected during the isothermal increase of the magnetic field followed by demagnetization show a pronounced metamagnetic behavior with hysteresis of $\mu_0 H=0.45$ T. The critical field changes linearly with temperature with $dH_{\text{cr}}/dT=0.25$ T/K, in good agreement with the $dT_C/dH=4.3$ K/T value obtained from the $M(T)$ data. The spontaneous magnetization (M_s) determined by linear extrapolation of $M(H)$ data collected at 2 K to $\mu_0 H=0$ T is 198.7 emu/g, which corresponds to an average magnetic moment of $7.50\mu_B$/Gd atom, in fair agreement with the theoretical gJ value of $7.0\mu_B$/Gd atom, and with the experimental value of pure Gd metal ($7.63\mu_B$/Gd atom).[52] The magnetic entropy change (magnetocaloric effect, MCE) ΔS_{mag} in the vicinity of MST in $Gd_5Si_{0.5}Ge_{3.5}$ determined from magnetization data for a magnetic field change from 0 to 5 T is −44 J/kg K, which is the largest known MCE value for a material which orders at ~80 K [the next best material is Gd_5Sn_4 ($T_C=82$ K) with a value of −38.5 J/kg K].[53]

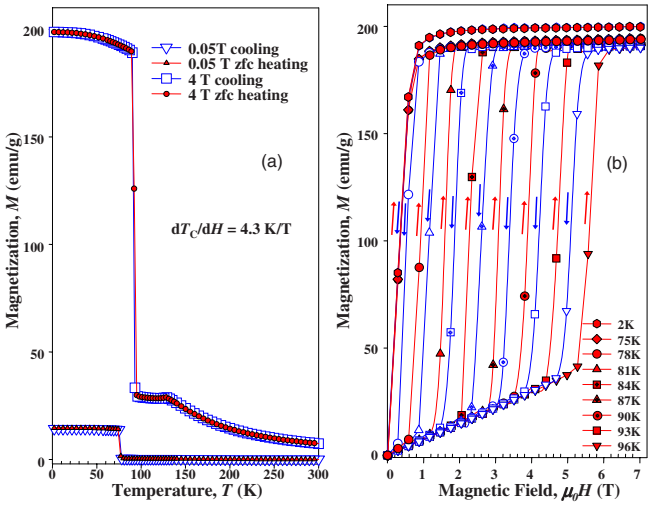

FIG. 1. (Color online) (a) Temperature and (b) magnetic field dependencies of the dc magnetization of $Gd_5Si_{0.5}Ge_{3.5}$ heat treated for 1 h at 1300 °C.

The results obtained for the as cast sample are basically the same, but with a few different features. Its Néel temperature remains the same, i.e., $T_N=130$ K. However, its Curie temperature is higher by 12 K ($T_C=89$ K) and the transition is slightly broader (~6 K) with a 2 K hysteresis. The reciprocal magnetic susceptibility $1/\chi_{\text{dc}}$ curves collected at $\mu_0 H=2$ and 4 T are identical to those of the heat-treated sample, but the $\mu_0 H=0.05$ T data show a remarkable Griffiths-phase-like behavior (a strong negative deviation from linearity) between T_N and ~250 K, which was not observed at this field in the heat-treated alloy. As cast sample has lower spontaneous magnetization at 2 K, $7.34\mu_B$/Gd. The latter is close to $7.35\mu_B$/Gd observed in $Gd_5Si_2Ge_2$.[54]

The origin of the higher T_C in the as cast alloy is not completely clear and is likely a combination of several factors. First, the transition temperature in this region of the Gd_5Si_4-Gd_5Ge_4 pseudobinary phase diagram is not only sensitive to the silicon content,[19,22] but it is also sensitive to the distribution of silicon and germanium atoms in the lattice, which may change during the heat treatment.[55] In fact, heat treatment always decreases T_C in $Gd_5Si_xGe_{4-x}$ compounds,[22,55,56] but such a strong (12 K) suppression has not been observed in the past. Furthermore, first-principles calculations show that atomic redistribution is an important factor in this case (see below). Second, by taking into account the lower value of the observed magnetic moment of Gd in the as cast alloy, it is possible that the phase composition of the as cast sample is somewhat different from the

annealed $Gd_5Si_{0.5}Ge_{3.5}$ due to intrinsic inhomogeneities, which may be present in the relatively large arc-melted buttons.

These assumptions are supported by experiments performed on microgram sized single crystals, which are commonly used for x-ray single crystal diffraction studies. These crystals, extracted from both as cast and heat-treated samples, were employed in x-ray single crystal diffractometer studies and then their magnetic properties were measured using the SQUID magnetometer. The measured signal was on the edge of the sensitivity of the magnetometer; however, the temperature of the transition can be clearly seen and the behavior of single crystals extracted from heat-treated and as cast buttons is different. The transition in the as cast crystal is broader, thus indicating its intrinsic inhomogeneity over the length scale of a few micrometers. According to the x-ray single crystal diffraction data, as cast crystals have a tendency toward concentrating Si in the interslab lattice sites in comparison with the heat-treated crystals. The MST temperature is also higher for the as cast crystal by ~10 K, which corresponds to the temperature difference in T_C of the bulk as cast and heat-treated samples. On the other hand, the site occupancies and compositions obtained using x-ray powder diffraction (see next section) of the as cast and heat-treated samples are within ~2% of one another (which is the accuracy of the calculations of the Si/Ge occupation). Thus, in addition to an atomic redistribution during the heat treatment and elimination of compositional inhomogeneities, there may be other factors responsible for the difference in the Curie temperatures of the as cast and annealed samples in $Gd_5Si_{0.5}Ge_{3.5}$ and other $Gd_5Si_xGe_{4-x}$ compounds. These include changes in local order, Griffiths-phase-like behavior (taking into account the difference between the $\mu_0 H = 0.05$ T data described above), and refinement of microstructure, all of which require further investigations.

The magnetic properties of the consolidated powdered sample extracted from the specimen used in the x-ray powder diffraction experiments show the same basic features as for the bulk samples, although the MST is much broader (it occurs over the range of ~15 K). At 2 K (and at 8 K), the isothermal magnetization measurements show a weak but measurable hysteresis, which was not observed in bulk samples (Fig. 2). The hysteresis disappears during the second and subsequent magnetization and demagnetization cycles. Such behavior is reflective of an incomplete structural transformation to O(I)-$Gd_5Si_{0.5}Ge_{3.5}$ during zero-field cooling observed from the x-ray data (see below) assuming that the magnetic field increases the degree of O(II)→O(I) conversion. However, the x-ray powder diffraction experiment carried out at $T=8$ K does not show an increase of the O(I)-phase content within 1% accuracy when the magnetic field is changed from 0 to 4 T. Hence, the origin of hysteresis is probably due to the rotation of some powder particles during the first magnetization cycle, despite the fact that the particles are bonded with varnish. During the magnetization process, some of them may twist to align the easy magnetization axis with the magnetic field vector, thus increasing net magnetization by a few percent. Once the particles that can move have found their most favorable positions, the hysteresis disappears.

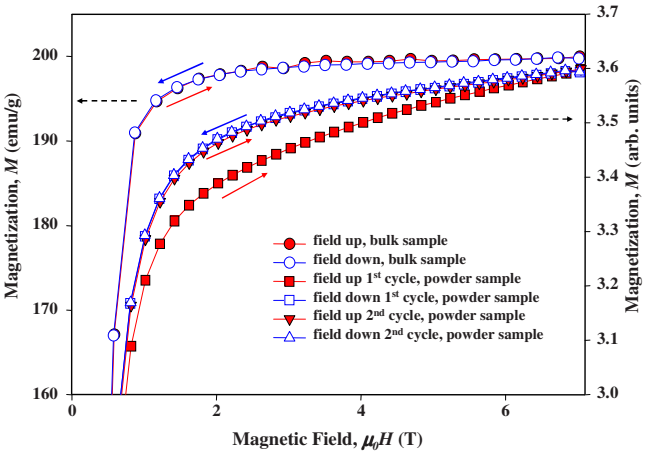

FIG. 2. (Color online) Isothermal dc magnetization of the bulk and powder samples of $Gd_5Si_{0.5}Ge_{3.5}$ alloy heat treated at 1300 °C for 1 h measured at 2 K. The measurement of powder sample includes two cycles of magnetization and demagnetization. Because the powder was mixed with GE varnish (see Refs. 26 and 40), the exact values of the magnetization are unknown and, thus, arbitrary units are used.

X-ray powder diffraction in $H=0$ T

The x-ray powder diffraction patterns of $Gd_5Si_{0.5}Ge_{3.5}$ heat treated at 1300 °C for 1 h were identical at temperatures ranging from 300 to 80 K except for a shift of Bragg peaks consistent with anisotropic thermal expansion, see below. The Rietveld refinement showed that the sample had the Sm_5Ge_4-type structure [O(II) phase] in this temperature range. At 80 K, additional Bragg peaks appeared, indicating a structural change in the sample. At 75 K and lower temperatures, these new Bragg reflections become dominant [Fig. 3(a)]. According to the Rietveld refinement, the new reflections correspond to the Gd_5Si_4-type structure [O(I) phase], confirming the expected[23] structural transition from the O(II)- to O(I)-$Gd_5Si_{0.5}Ge_{3.5}$ at temperatures below 80 K. Below 65 K, the powder diffraction patterns remain characteristic of Gd_5Si_4-type structure down to 8 K (the lowest temperature of the x-ray experiment).

On heating, the reverse structural transformation from the O(I)-type structure to the O(II)-type structure can be observed at slightly higher temperatures than during the cooling; it starts at 70 K and ends at 85 K [Fig. 3(b)]. The change of the concentration of the low-temperature Gd_5Si_4-type phase with temperature during both cooling and heating is presented in Fig. 4. A hysteresis of 5 K is noticeable. The transition on cooling is incomplete with nearly 92% of the O(II)-$Gd_5Si_{0.5}Ge_{3.5}$ transforming into the O(I) allotrope at 8 K. It is worth noting that the phase coexistence (or phase separation) in $Gd_5Si_xGe_{4-x}$ alloys is a common phenomenon observed by means of both powder[25,40] and single crystal[57] x-ray diffraction methods. The reasons of an incomplete transformation in $Gd_5Si_{0.5}Ge_{3.5}$ should be similar to those in polycrystalline Gd_5Ge_4 samples,[40] and, most probably, the transformation remains incomplete due to the presence of structural defects and inhomogeneities in the specimen. Structural disorder has already been associated with broad-

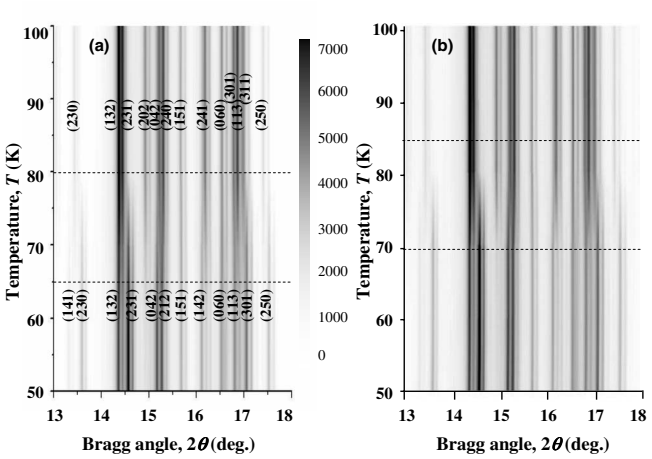

FIG. 3. The intensity contour maps of the x-ray powder diffraction patterns of $Gd_5Si_{0.5}Ge_{3.5}$ collected in zero magnetic field during (a) cooling and (b) heating. All patterns were collected using Mo $K\alpha$ radiation. Only the ranges between 13° and 18° of 2θ and between 50 and 100 K are shown for clarity. The bar between the two plots represents the intensity scale. The crystallographic Miller indices are shown for the most intense Bragg reflections in (a). The dashed horizontal lines represent the beginning and the end of the transformation.

ening of first-order structural transformations, and a large amount of local defects can lead to phase coexistence over a broad range of thermodynamic variables partially transforming a first-order transition into a second-order one.[18,58–60] A disorder should increase during grinding and mechanical fracturing of an alloy, and in a powder sample, the completeness of transformation is reduced.

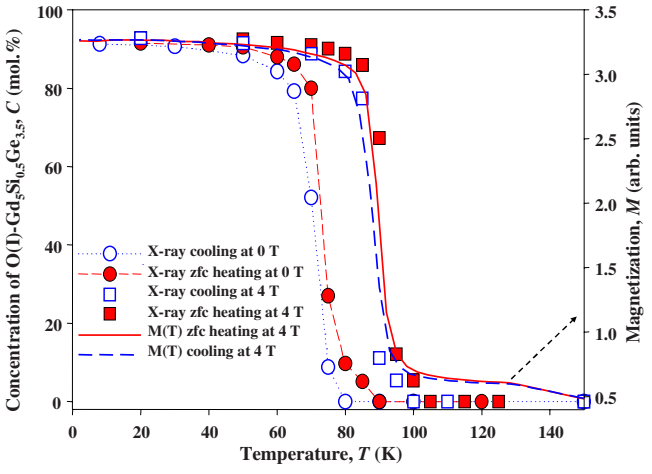

FIG. 4. (Color online) The molar concentration of the O(I)-$Gd_5Si_{0.5}Ge_{3.5}$ phase (symbols, left hand scale) determined from x-ray powder diffraction measurements during heating and cooling in $\mu_0 H=0$ and 4 T fields as function of temperature, and the dc magnetization of the heat-treated $Gd_5Si_{0.5}Ge_{3.5}$ powder sample measured in $\mu_0 H=4$ T magnetic field (thick lines, right hand scale) during heating and cooling. Arbitrary units are used because the powder was mixed with varnish (see experimental procedure) and its exact mass was unknown.

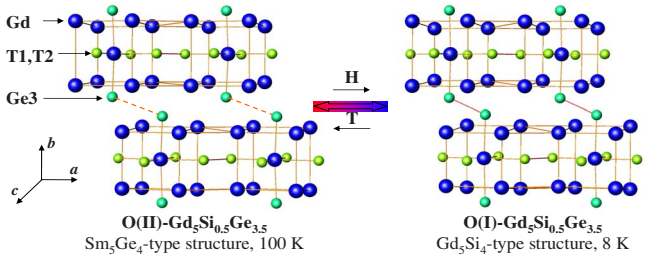

FIG. 5. (Color online) The connectivity of neighboring slabs in Sm_5Ge_4- and Gd_5Si_4-type polymorphs of $Gd_5Si_{0.5}Ge_{3.5}$. The long (3.62 Å) interslab Ge3–Ge3 bonds are shown with the dashed lines, whereas the short (2.75 Å) Ge3–Ge3 bonds are shown with the solid lines.

The crystallographic data for both allotropic modifications of $Gd_5Si_{0.5}Ge_{3.5}$ are presented in Table I. The structural parameters of the O(I) phase are shown for $T=8$ K, and of the O(II) phase for $T=100$ K; these data were used to model the structures for first-principles calculations. Following the Rietveld refinement, the T1 and T2 positions, which are the intraslab sites in our notation, are occupied by a mixture of tetrelide atoms, and, within the experimental errors, the Si/Ge ratio is the same for both T1 and T2. The interslab T3 site is fully occupied by Ge, thus it is denoted as the Ge3 site. The composition calculated from the x-ray data is nearly identical to the nominal $Gd_5Si_{0.5}Ge_{3.5}$ composition. The distribution of Si/Ge atoms is in agreement with previous reports on $Gd_5Si_xGe_{4-x}$ alloys where the smaller (Si) atoms prefer the intraslab sites and the larger (Ge) atoms prefer the interslab positions.[57,61] This is different from Ref. 23, where three crystallographically independent sites were assumed to be evenly occupied by 10% Si and 90% Ge. Overall, the accuracy of our crystallographic data is much higher than that reported in Ref. 23. The connectivity of neighboring slabs in both $Gd_5Si_{0.5}Ge_{3.5}$ polymorphs is illustrated in Fig. 5. The atomic arrangement within the slabs is practically identical for both structures: when one structure transforms into another, the average change of the intralayer atomic distances is less than 2%. However, the distances between the atoms from the neighboring layers change drastically, and the average value of this change is about 15%. Therefore, the displacive shift of the atomic layers determines the mechanism of the O(I)↔O(II) transition.

The interslab Ge3–Ge3 bonds in the Gd_5Si_4-type structure break upon transition to the Sm_5Ge_4-type structure as evidenced by the elongation of the Ge3–Ge3 interatomic distances by ~32%: from $d_{Ge3-Ge3}=2.75(1)$ Å in the former, which is close to the sum of the Ge atomic radii [$r_{Ge}=1.378$ Å (Ref. 62)], to $d_{Ge3-Ge3}=3.62(1)$ Å in the latter, which indicates no direct bonding between these atoms (Fig. 6). It is worth noting that the Ge3–Ge3 distance relaxes gradually in the Gd_5Si_4-type polymorph during both heating and cooling. However, unlike in the O(II) polymorph of $Gd_5Si_{0.4}Ge_{3.6}$, where the interslab Ge3–Ge3 distance was reported[23] to vary gradually, the title compound exhibits a spike at the top of the step both on heating and cooling just above the transition. Thus, the longest Ge3–Ge3 distance, $d_{Ge3-Ge3}=3.73(2)$ Å, is observed in zero magnetic field at

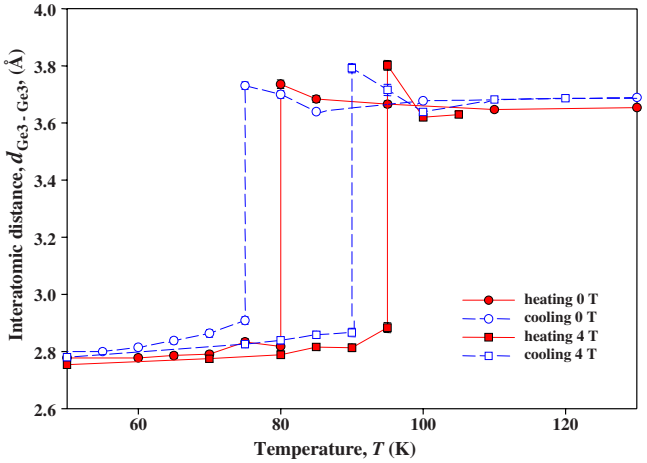

FIG. 6. (Color online) Temperature dependencies of the Ge-Ge interslab bond distances, $d_{Ge3-Ge3}$, determined from x-ray powder diffraction measurements during heating and cooling in $\mu_0 H=0$ and 4 T applied magnetic fields.

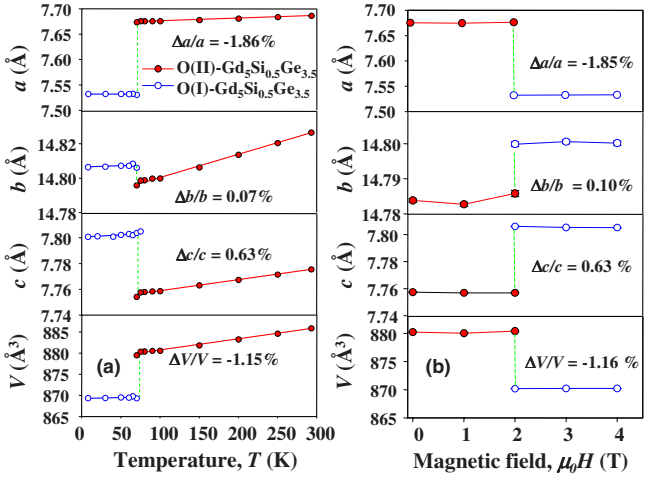

FIG. 7. (Color online) Lattice parameters of $Gd_5Si_{0.5}Ge_{3.5}$ (both Sm_5Ge_4-type and Gd_5Si_4-type phases) determined from x-ray powder diffraction measurements of the heat-treated sample during (a) cooling in $\mu_0 H=0$ T and (b) isothermal magnetization at $T=80$ K. The standard deviations for the parameters are not shown on the plot because they are smaller than symbol sizes.

80 K, but at 90 K it reaches a stable value of 3.62(1) Å, which, on heating, only slightly (and gradually) increases to 3.68(1) Å at room temperature. This observation points to a special role of Ge3–Ge3 bonding in the O(I)↔O(II) transition because other interatomic distances do not show such a distinct behavior. However, spikes in Ge3–Ge3 interatomic distance near the transition do not exist when the magnetic field is the driving force of the transformation (see below). According to the Rietveld refinement, the atomic positions change little with temperature approximately 30 K above and below the transition temperature.

The change of lattice parameters of both phases with temperature and applied magnetic field was calculated using Rietveld refinement of the x-ray powder patterns. Only the results on cooling are shown in Fig. 7(a) for clarity, because the values of the lattice parameters during heating are the same, except for a 5 K displacement of the discontinuities due to thermal hysteresis. The standard deviations for the parameters are not shown in the plots because they are smaller than symbol sizes. All lattice parameters decrease linearly when temperature decreases from 300 to 100 K, and the coefficients of linear thermal expansion along the three crystallographic axes are $\alpha_a=7.9\times10^{-6}$ K^{-1}, $\alpha_b=12.7\times10^{-6}$ K^{-1}, and $\alpha_c=11.4\times10^{-6}$ K^{-1}. The latter are similar to those observed in Gd_5Ge_4,[63] i.e., $\alpha_a=6.9\times10^{-6}$ K^{-1}, $\alpha_b=11.8\times10^{-6}$ K^{-1}, and $\alpha_c=10.3\times10^{-6}$ K^{-1}, both in their absolute values and anisotropy. No anomalies of thermal expansion were noted around $T_N=130$ K, similar to Gd_5Ge_4.[40] In the region of the phase transformation, the abrupt changes in the lattice dimensions are observed due to the O(I)↔O(II) transition. Below the transition, b- and c-lattice parameters do not change from 8 to 50 K, and only above 50 K do they begin to slowly expand. The a parameter remains constant to within three standard deviations for the low-temperature phase. The discontinuous changes of the lattice parameters during the transition follow the pattern previously observed for other $Gd_5Si_xGe_{4-x}$ compounds. The large decrease in the a parameter ($\Delta a/a=-1.86\%$) is consistent with the shear displacement of atomic layers along a during the structural transition between Gd_5Si_4 and Sm_5Ge_4 types. The opposite changes observed along the other two directions are significantly smaller: $\Delta c/c=0.63\%$ and $\Delta b/b=0.07\%$. As a result, the unit-cell volume change is quite large ($\Delta V/V=-1.16\%$) and is mainly determined by the contraction along the a axis. The observed unit-cell discontinuities agree well with $\Delta a/a=-1.6\%$, $\Delta b/b=0.3\%$, and $\Delta c/c=0.7\%$ values reported for $Gd_5Si_{0.4}Ge_{3.6}$.[23] It is worth noting that the direction along which the main change occurs during the transition, which is the a axis, has the smallest linear thermal expansion coefficient, α_a, whereas the direction of the smallest change, the b axis, has the largest α.

X-ray powder diffraction in applied magnetic fields

In addition to zero magnetic field measurements, x-ray powder diffraction patterns were collected at temperatures ranging from 20 to 150 K in a constant dc magnetic field of $\mu_0 H=4$ T for both as cast and heat-treated samples. The obtained results, in general, follow the x-ray experiments without the magnetic field, with an increase of the transformation temperature (during cooling and heating) by ~16 K (Fig. 4), in full correspondence with the magnetic measurements of the same powder sample, which was used in the x-ray experiments. The temperature of the structural transition increases with a rate of ~4 K/T, and thermal hysteresis remains about 5 K wide. The changes of the lattice parameters and the unit-cell volume with temperature are similar to those observed at $\mu_0 H=0$ T with the same 16 K shift of their values to higher temperature. A slight broadening of the transition range was observed in comparison with the measurements without the magnetic field. The change of the O(I)-phase content with temperature matches the magnetiza-

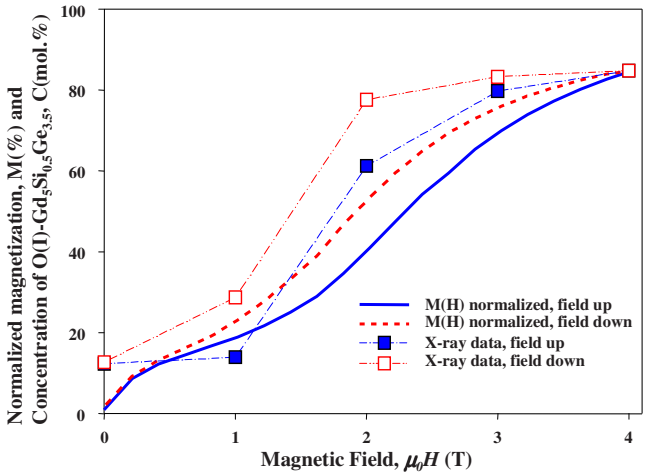

FIG. 8. (Color online) The normalized magnetization of $Gd_5Si_{0.5}Ge_{3.5}$ shown in % of the magnetization of this sample at $T=80$ K and $\mu_0 H=4$ T (lines), and molar concentration of the O(I) phase (symbols) determined from magnetization and x-ray powder diffraction measurements during isothermal magnetization and demagnetization at $T=80$ K.

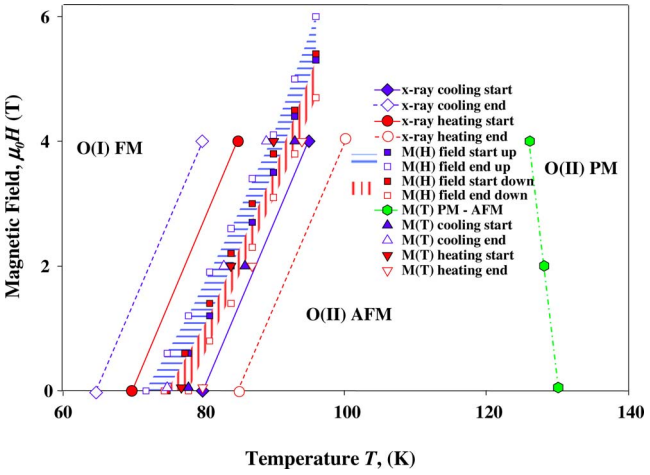

FIG. 9. (Color online) The H-T phase diagram of $Gd_5Si_{0.5}Ge_{3.5}$. The area shaded with vertical lines (red) corresponds to the region of MST during demagnetization and heating, and the area shaded with horizontal lines (blue) reflects the region of the transition during magnetization and cooling.

tion $M(T)$ data obtained for the $Gd_5Si_{0.5}Ge_{3.5}$ powder (Fig. 4) at $\mu_0 H=4$ T and confirms the intimate coupling between the crystal structure and magnetic ordering in this compound. The discrepancy seen above T_C is due to the nonzero magnetization of the AFM phase in the 4 T magnetic field.

Isothermal magnetization experiment was performed at $T=8$ and 80 K by varying the field from 0 to 4 T and back from 4 to 0 T in 1 T steps. At the beginning of the experiment performed at $T=80$ K, the sample was cooled to 20 K in zero magnetic field and then warmed up to $T=80$ K. The Rietveld refinement shows no structural difference at $\mu_0 H=0$ and 4 T at $T=8$ K: both the lattice parameters and phase contents remain identical. At $T=80$ K, an increase of the magnetic field results in the increase of the concentration of the low-temperature phase from 12 to 85 mol % (Fig. 8). The demagnetization shows a noticeable hysteresis, but at 0 T, the concentration of the low-temperature phase returns to the 12 mol % value recorded before magnetization. The changes in the lattice parameters of each phase during isothermal magnetization and demagnetization are negligible—the values of the lattice parameters and unit-cell volumes are within three standard deviations from one another. This is consistent with the expected negligible conventional magnetostriction expected for an S-state Gd^{3+} ion. However, the magnetostriction due to a structural change from O(I) to O(II) is significant. The values obtained during the magnetization of $Gd_5Si_{0.5}Ge_{3.5}$ are shown in Fig. 7(b).

The $M(H)$ data for the same powder sample, which was used in the x-ray experiment, were collected from 0 to 4 T range and normalized using the formula $M=M_0/M(80\ \mathrm{K},4\ \mathrm{T})\times C_{\mathrm{O(I)}}(80\ \mathrm{K},4\ \mathrm{T})$, where M is magnetization and $C_{\mathrm{O(I)}}$ is concentration of the O(I) phase. They are shown in Fig. 8 together with the x-ray isotherm. The magnetization follows the concentration of the O(I) phase, as in the case of the temperature-dependent measurements shown in Fig. 4. There is, however, a small discrepancy in values between the x-ray and magnetic data, which, we believe, originates from the following reasons: (a) the normalization provides a certain error due to incompleteness of the transition, and (b) intrinsic difference between the x-ray and dc magnetization measurements. In the magnetization experiment, a measured signal reflects a structural change as well as the alignment of magnetic domains and magnetic moments, whereas the x-ray experiment is only sensitive to a structural change. Consequently, in the magnetization measurement, a certain magnetic field is needed first to rotate domains, and only then the concentration of the FM phase would be reflected by the total magnetization value. In addition, both of the coexisting AFM and/or PM phases have nonzero magnetizations in nonzero magnetic fields.

The changes in the Ge3–Ge3 interatomic distances during the isofield measurements are similar to those observed for nonmagnetic heating and cooling, and they are shifted to higher temperatures with ~4 K/T rate (Fig. 6). However, there are no pre- and post-transition anomalies in the Ge3-Ge3 interslab distances during isothermal magnetization or demagnetization at $T=80$ K, so these appear to be temperature-dependent phenomena. This fact is intriguing because it indicates that the lattice behavior near the transition depends on whether the latter is triggered by temperature or magnetic field. The difference is probably related to the fact that in $Gd_5Si_{0.5}Ge_{3.5}$ the temperature change does affect the lattice dimensions and volume because of thermal expansion, whereas the magnetic field does not induce conventional magnetostriction in either of the polymorphic modifications.

The compilation of the results of the magnetic measurements of the bulk sample and x-ray powder diffraction studies is presented in the magnetic field (H)–temperature (T) phase diagram of the heat-treated $Gd_5Si_{0.5}Ge_{3.5}$ (Fig. 9). The region of the structural transformation determined from x-rays is broader than the region of the magnetic transition (shading with the red vertical lines represents transition

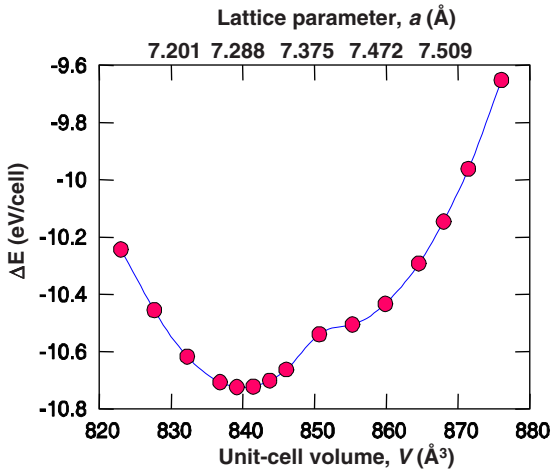

FIG. 10. (Color online) Total energy variation in FM $Gd_5Si_{0.5}Ge_{3.5}$ as a function of lattice parameter a and unit-cell volume. The global minimum at 840 Å^3 corresponds to the O(I) phase, and the local minimum at 855 Å^3 corresponds to the O(II) phase.

range during demagnetization and heating, and the blue horizontal lines represent the same during magnetization and cooling) due to the broadening of the transition in a powder. The characteristic features of this diagram are low hysteresis associated with the MST in the magnetic data and a negative shift of the Néel temperature with applied magnetic field. A linear extrapolation of the phase boundaries shows that in magnetic fields of $\mu_0 H \cong 10$ T and higher, the AFM state would be completely suppressed and the magnetostructural transition would occur directly between O(I) FM and O(II) PM states. Approximate coordinates of the tricritical point are estimated to be $\mu_0 H = 10$ T and $T = 120$ K.

THEORETICAL AND COMPUTATIONAL RESULTS AND DISCUSSION

In order to verify the first-order nature of the magnetostructural phase transformation in $Gd_5Si_{0.5}Ge_{3.5}$, first-principles theory was employed to calculate the total energy as a function of unit-cell volume. This is one of the ways to check whether there is only one state or if a metastable state, which is separated by the energy barrier from the known ground state, exists. Figure 10 shows total energy variation with respect to unit-cell volume. Here, volume change was modeled by varying lattice parameter a while keeping constant lattice parameters $b = 14.785$ Å and $c = 7.796$ Å, which are the lattice parameters of O(I) phase at 8 K, and do not substantially change from the O(II) phase (see Table I). The low-temperature O(I) structure has been used in these calculations because it represents experimentally known ground state. The lattice constant a was varied because the change in a determines the sign of volume effect (see Fig. 7). Even though changing a without gradually changing the coordinates of atoms does not represent a real structural change between the O(II) and O(I) phases, this approximation may be useful in probing the effect of volume change on the nature of the phase transformation. Parallel (FM) spin arrangement of Gd atoms as in the ground state of the compound was assumed. The global total energy minimum in Fig. 10 corresponds to the O(I) phase. A metastable state occurs at 15 Å^3 higher than the global equilibrium volume. This metastable state corresponds to the O(II) structure because the volume difference between the global and local total energy minima agrees well with the experimentally determined volume difference of 11 Å^3 between the O(I) and O(II) $Gd_5Si_{0.5}Ge_{3.5}$ near the transition. This result, therefore, confirms the first-order nature of the phase transformation between the O(I) and O(II) structures. It also indicates that phase volume alone is an important factor in stabilizing either of the two structures in this compound, as has been recently shown from pressure-dependent experiments.[64] It is worth noting here that, in Gd_5Ge_4, O(II) is ground state and it transforms to O(I) when magnetic field is applied. However, in $Gd_5Si_{0.5}Ge_{3.5}$, the ground state is O(I) as shown in Fig. 10. It happens because Si prefers the low-volume O(I) structure as the stable state under the condition of chemical pressure caused by the size difference between Si and Ge atoms. It should also be noted here that the calculated equilibrium volumes are underestimated by ~3% compared to the corresponding experimental values. This is not unusual because the LSDA+U approach often underestimates the experimental unit-cell volume. The energy barrier between these two states is 0.186 eV/cell (see Fig. 10).

Considering that the O(II) $Gd_5Si_{0.5}Ge_{3.5}$ is experimentally observed to be AFM in the temperature range from 77 to 130 K, total energy for the AFM spin arrangement between the slabs has also been calculated. It is lower by 0.214 eV/cell than that for the FM O(II) $Gd_5Si_{0.5}Ge_{3.5}$. This AFM structure was constructed by doubling the unit cell in the b direction and assigning ↑↑ (spin up) configurations to Gd atoms in one slab and ↓↓ (spin down) configurations in the neighboring slabs. Using the total energy difference per Gd atom between the AFM and FM spin arrangements, an estimate of the FM-AFM transition temperature (T_M) can be made using the mean field relationship

$$T_M = \frac{2}{3}\left(\frac{E_{FM} - E_{AFM}}{K_B}\right).$$

The calculated value of T_M is 83 K, which is close to the experimentally observed value of $T_C = 77$ K (see Fig. 1).

In order to evaluate the difference in the magnetism between the O(I) and O(II) $Gd_5Si_{0.5}Ge_{3.5}$, the local exchange splitting can be computed as a difference of the respective potential parameters (C) at the center of the atom projected bands. This local splitting causes an exchange splitting in the majority and minority spin bands, giving rise to the 5d magnetic moments of Gd atoms. The calculated 5d local exchange splittings for Gd1, Gd2, and Gd3 of the O(I) phase are 1.58 (1.56) eV, 1.36 (1.34) eV, and 1.35 (1.33) eV, respectively, assuming a FM spin alignment, and that the T1 and T2 positions are occupied by Ge (or Si, values in parentheses) atoms. The corresponding values of FM O(II) $Gd_5Si_{0.5}Ge_{3.5}$ are lower: 1.25 (1.27) eV, 1.13 (1.14) eV, and 1.17 (1.17) eV, respectively. Thus, the O(I) structure is more

TABLE II. Spin magnetic moments (in μ_B) of different Gd atoms in the FM O(I) and FM O(II) $Gd_5Si_{0.5}Ge_{3.5}$. The values in parentheses denote the magnetic moments when T1 and T2 positions are occupied by Si atoms.

	6*s*	6*p*	5*d*	4*f*	Total
			O(I) $Gd_5Si_{0.5}Ge_{3.5}$		
Gd1	0.02 (0.02)	0.06 (0.07)	0.53 (0.51)	6.98 (6.97)	7.59 (7.57)
Gd2	0.02 (0.03)	0.04 (0.04)	0.41 (0.40)	6.99 (6.97)	7.46 (7.44)
Gd3	0.02 (0.02)	0.04 (0.05)	0.35 (0.33)	6.97 (6.97)	7.38 (7.37)
			O(II) $Gd_5Si_{0.5}Ge_{3.5}$		
Gd1	0.01 (0.02)	0.05 (0.05)	0.31 (0.30)	6.98 (6.98)	7.35 (7.35)
Gd2	0.01 (0.01)	0.01 (0.01)	0.23 (0.23)	6.97 (6.97)	7.23 (7.23)
Gd3	0.01 (0.01)	0.02 (0.02)	0.21 (0.20)	6.97 (6.95)	7.20 (7.18)

favorable for higher magnetic moments than the O(II) structure.

In Table II, the magnetic moments due to outer *s*, *p*, *d*, and *f* electrons as well as total moments are shown for Gd atoms in the FM $Gd_5Si_{0.5}Ge_{3.5}$. As expected, magnetic moments due to *f* electrons are close to $7\mu_B$, and the moments due to *s* and *p* electrons are negligible when compared to *d* and *f* electrons. The main differences in the magnetic moments are in the 5*d* electrons of the different Gd atoms in both the O(I) and O(II) $Gd_5Si_{0.5}Ge_{3.5}$ phases. The larger values of 5*d* moments in the O(I) structure are due to the higher spin polarization in this structure as compared to the O(II) structure, which is reflected in the Gd 5*d* density of states (DOS) described later. The calculated average magnetic moment is $7.48\mu_B$/Gd atom for the O(I) structure, matching the experimental observation of the saturated magnetic moment in O(I) at 2 K, which is $7.50\mu_B$/Gd atom, and $7.24\mu_B$/Gd atom for the O(II) structure. It is reasonable to argue that the reduction in 5*d* moment by 50% as compared to the FM O(I) structure is responsible for weakening the indirect Ruderman-Kittel-Kasuya-Yosida coupling between Gd 4*f* moments in the neighboring slabs, which is enough to prevent the O(II) FM state being stable over the O(II) AFM or PM state. As will be shown below, a dramatic difference in the hybridization between 5*d* electrons of Gd1 and 4*p* electrons of Ge3 depends on whether the short Ge3–Ge3 pairs as in the O(I) structure or the long Ge3–Ge3 pairs as in the O(II) structure are formed; these interslab bonds being primarily responsible for the difference in the interslab coupling in the O(I) and O(II) structures.

In order to probe how the structural change affects the electronic structure and magnetism of $Gd_5Si_{0.5}Ge_{3.5}$, the Gd 5*d* and Ge 4*p* DOS were calculated with the FM order imposed in both the O(I) and O(II) structures. Figure 11 shows that 5*d* DOS of symmetrically inequivalent Gd atoms in the FM O(I) and FM O(II) $Gd_5Si_{0.5}Ge_{3.5}$ are different at the Fermi level. On average, the spin up DOS at the Fermi level of these Gd atoms in the FM O(I) structure is higher by 25% than that in the FM O(II) structure. The corresponding average spin down DOS at the Fermi level is almost identical in both structure types. The 5*d* band splitting at the Fermi level for the O(I) structure is higher by 16% than for the O(II) structure, resulting in a higher average 5*d* magnetic moments mentioned above.

It is interesting to note here that the average spin up DOS of Gd atoms at the Fermi level in the FM O(I) structure is higher by 12% when Si atoms occupy T1 and T2 sites compared to Ge atoms occupying these sites. On the other hand, the average spin up DOS of Gd atoms at the Fermi level in the FM O(II) structure is lower by 3% when placing Si atoms in T1 and T2 sites compared to Ge atoms in these sites. This observation indicates that intraslab Si atoms in T1 and T2 sites enhance the ferromagnetism in the O(I) structure but not in the O(II) structure of $Gd_5Si_{0.5}Ge_{3.5}$. We point out that in the O(I) and O(II) structures of silicon-free analog—Gd_5Ge_4—the intraslab magnetic coupling between the Gd atoms is similar, but the interslab magnetic coupling is different.[38] Here, because of the presence of silicon in the T1 and T2 sites in $Gd_5Si_{0.5}Ge_{3.5}$, the intraslab ferromagnetic coupling between Gd atoms of the O(I) $Gd_5Si_{0.5}Ge_{3.5}$ is enhanced, but the interslab coupling is similar to that in Gd_5Ge_4. Hence, the enhancement of the intraslab ferromagnetic coupling due to Si must be the origin of the higher values of the magnetostructural transition temperature in the $Gd_5S_xGe_{4-x}$ system as *x* increases. It should also be noted

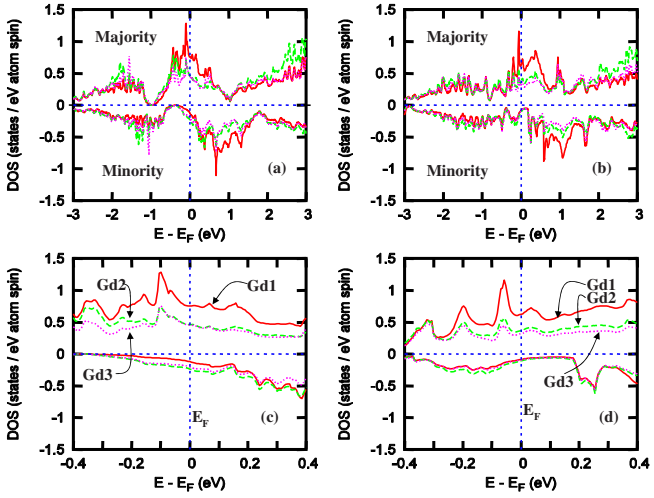

FIG. 11. (Color online) The 5*d* DOS of symmetrically inequivalent Gd atoms in (a) the O(I) phase and (b) the O(II) phase of $Gd_5Si_{0.5}Ge_{3.5}$. For clarity, the regions near the Fermi level are enlarged for (c) the O(I) phase and (d) the O(II) phase.

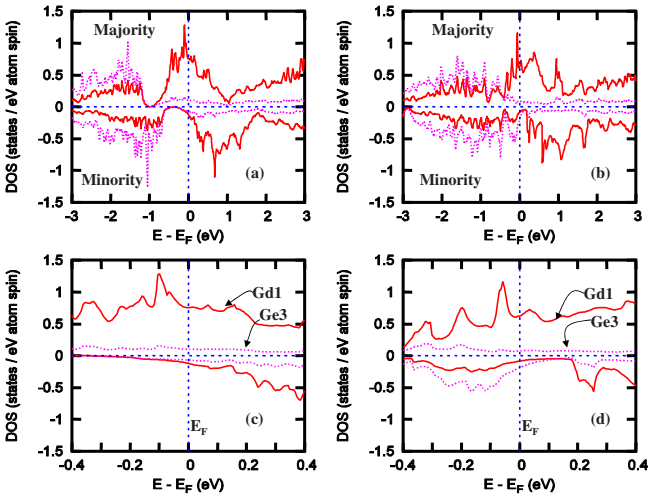

FIG. 12. (Color online) The 5*d* DOS of Gd1 and 4*p* DOS of Ge3 in (a) the O(I) phase and (b) the O(II) phase of $Gd_5Si_{0.5}Ge_{3.5}$. For clarity, the regions near the Fermi level are enlarged for (c) the O(I) phase and (d) the O(II) phase.

that the average spin up 5*d* DOS of Gd atoms at the Fermi level in the FM O(II) structure is higher by 2.5% with Ge atoms between the slabs (Ge3 sites) and Si atoms inside the slabs (T1 and T2 sites) compared to Si outside and Ge inside the slabs. This indicates that if some of the interslab Ge3 sites of $Gd_5Si_{0.5}Ge_{3.5}$ are occupied by Si atoms in the O(II) structure (as observed experimentally in single crystals extracted from a non-heat-treated alloy), then the spin up 5*d* DOS at the Fermi level decreases slightly, resulting in a small decrease in the magnetic moment due to 5*d* electrons of Gd atoms.

Since Gd1 atoms from one slab are connected to Gd1 atoms from the neighboring slabs either through the short Ge3–Ge3 pairs in the O(I) or through the long Ge3–Ge3 pairs in the O(II)-type $Gd_5Si_{0.5}Ge_{3.5}$, the difference in the overlap between the 5*d* states of Gd1 and 4*p* states of Ge3 should be responsible for the difference in the interslab coupling in these structure types. This is seen in the 5*d* DOS of Gd1 and 4*p* DOS of Ge3 in both structures, which are compared in Fig. 12. The spin up and spin down 4*p* DOS of Ge3 atom are almost identical at the Fermi level in the O(I) structure, indicating 50% Gd1 5*d* and 50% Ge3 4*p* hybridization in the same spin down, band while for the O(II) structure, the spin down 4*p* DOS of Ge3 atom is larger at the Fermi level, indicating 30% Gd1 5*d* and 70% Ge3 4*p* hybridization. This shows that Ge3 atoms in the O(I) do not reduce the magnetic moment of Gd atoms surrounding Ge3 sites. The spin down 4*p* states of Ge in the O(II) have been pushed toward the Fermi level because of the weak Ge3–Ge3 bonding, thus reducing magnetic moment on Gd atoms surrounding Ge3 sites. These results are consistent with the respective structures in the Gd_5Ge_4 system.[38]

SUMMARY

As expected, the $Gd_5Si_{0.5}Ge_{3.5}$ compound undergoes two transformations while cooling from room temperature to 2 K. At 130 K, the paramagnetic state transforms into an antiferromagnetic state via a second-order phase transition without any detectable structural change. At 77 K, the magnetic order-order transition (AFM to FM) takes place simultaneously with the first-order structural transformation from the high-temperature Sm_5Ge_4-type [O(II)] structure into the low-temperature Gd_5Si_4-type [O(I)] structure, similar to the previously reported first-order transitions in $Gd_5Si_{0.4}Ge_{3.6}$ and Gd_5Ge_4. Unlike the Gd_5Ge_4, the applied magnetic field is not necessary to cause of the AFM-FM transition in $Gd_5Si_{0.5}Ge_{3.5}$. The role of the magnetic field is played by the Si atoms, which exert chemical pressure in this material. The as cast alloy has a higher magnetostructural transition temperature (T_C=89 K) and a lower spontaneous magnetic moment at 2 K. A broader transition with noticeable hysteresis was observed in powder samples. During the transition, the average change of distances between atoms that belong to neighboring slabs by far exceeds that between atoms that belong to the same slab, thus highlighting the stability of the slabs. While the behavior of lattice parameters is always the same regardless of the nature of the trigger (temperature or magnetic field) initiating the magnetostructural transition, the behavior of the interslab Ge3–Ge3 distances is not the same: a spike in Ge3–Ge3 bond length is observed near the transition triggered by temperature, but not when it is driven by the magnetic field. The *H-T* phase diagram of $Gd_5Si_{0.5}Ge_{3.5}$ resembles the main features of previously reported Gd_5Ge_4 (Ref. 24) and shows that the AFM state can be fully quenched in $Gd_5Si_{0.5}Ge_{3.5}$ by a magnetic field as low as ~10 T at T=120 K.

The total energy vs unit-cell volume behavior confirms a first-order phase transformation between the O(II)-$Gd_5Si_{0.5}Ge_{3.5}$ and O(I)-$Gd_5Si_{0.5}Ge_{3.5}$, in agreement with the experiment. The 5*d* local exchange splitting of the Gd atoms in the O(I) $Gd_5Si_{0.5}Ge_{3.5}$ is larger than in the O(II) $Gd_5Si_{0.5}Ge_{3.5}$, resulting in higher 5*d* moments of Gd atoms in the O(I) $Gd_5Si_{0.5}Ge_{3.5}$ as compared to the O(II) $Gd_5Si_{0.5}Ge_{3.5}$. The differences in the Ge3 4*p* density of states in the O(I) and O(II) structures correlate with the differences of the Ge3–Ge3 bonding in these two structure types.

ACKNOWLEDGMENTS

This work was supported by the Office of Basic Energy Sciences, Materials Sciences Division of the U.S. Department of Energy under Contract No. DE-AC02-07CH11358 with Iowa State University of Science and Technology. The authors thank A.O. Tsokol for providing some of the samples, and Sumohan Misra for his help with x-ray single crystal examination.

*Corresponding author; vitkp@ameslab.gov

[1] V. K. Pecharsky and K. A. Gschneidner, Jr., Phys. Rev. Lett. **78**, 4494 (1997).
[2] L. Morellon, P. A. Algarabel, M. R. Ibarra, J. Blasco, B. Garcia-Landa, Z. Arnold, and F. Albertini, Phys. Rev. B **58**, R14721 (1998).
[3] L. Morellon, J. Stankiewicz, B. Garcia-Landa, P. A. Algarabel, and M. R. Ibarra, Appl. Phys. Lett. **73**, 3462 (1998).
[4] J. Stankiewicz, L. Morellon, P. A. Algarabel, and M. R. Ibarra, Phys. Rev. B **61**, 12651 (2000).
[5] E. M. Levin, V. K. Pecharsky, and K. A. Gschneidner, Jr., Phys. Rev. B **63**, 174110 (2001).
[6] J. B. Sousa, M. E. Braga, F. C. Correía, F. Carpinteiro, L. Morellon, P. A. Algarabel, and M. R. Ibarra, Phys. Rev. B **67**, 134416 (2003).
[7] F. Casanova, A. Labarta, X. Battle, F. J. Pérez-Reche, E. Vives, L. Mañosa, and A. Planes, Appl. Phys. Lett. **86**, 262504 (2005).
[8] J. B. Sousa, A. M. Pereira, F. C. Correía, J. M. Teixeira, J. P. Araujo, R. P. Pinto, M. E. Braga, L. Morellon, P. A. Algarabel, C. Magen, and M. R. Ibarra, J. Phys.: Condens. Matter **17**, 2461 (2005).
[9] E. M. Levin, A. O. Pecharsky, V. K. Pecharsky, and K. A. Gschneidner, Jr., Phys. Rev. B **63**, 064426 (2001).
[10] M. Manekar, M. K. Chattopadhyay, R. Kaul, V. K. Pecharsky, and K. A. Gschneidner, Jr., J. Phys.: Condens. Matter **18**, 6017 (2006).
[11] F. Casanova, A. Labarta, X. Batlle, E. Vives, J. Marcos, L. Mañosa, and A. Planes, Eur. Phys. J. B **40**, 427 (2004).
[12] V. Hardy, S. Majumdar, S. Crowe, M. R. Lees, D. M. Paul, L. Hervé, A. Maignan, S. Hébert, C. Martin, C. Yaicle, M. Herviue, and B. Raveau, Phys. Rev. B **69**, 020407 (2004).
[13] F. Casanova, A. Labarta, and X. Batlle, Phys. Rev. B **72**, 172402 (2005).
[14] J. Leib, J. E. Snyder, T. A. Lograsso, D. Schlagel, and D. C. Jiles, J. Appl. Phys. **95**, 6915 (2004).
[15] J. D. Moore, G. K. Perkins, Y. Bugoslavsky, M. K. Chattopadhyay, S. B. Roy, P. Chaddah, V. K. Pecharsky, K. A. Gschneidner, Jr., and L. F. Cohen, Appl. Phys. Lett. **88**, 072501 (2006).
[16] J. D. Moore, G. K. Perkins, Y. Bugoslavsky, L. F. Cohen, M. K. Chattopadhyay, S. B. Roy, P. Chaddah, K. A. Gschneidner, Jr., and V. K. Pecharsky, Phys. Rev. B **73**, 144426 (2006).
[17] F.-J. Pérez-Reche, F. Casanova, E. Vives, L. Mañosa, A. Planes, J. Marcos, X. Batlle, and A. Labarta, Phys. Rev. B **73**, 014110 (2006).
[18] S. B. Roy, M. K. Chattopadhyay, P. Chaddah, J. D. Moore, G. K. Perkins, L. F. Cohen, K. A. Gschneidner, Jr., and V. K. Pecharsky, Phys. Rev. B **74**, 012403 (2006).
[19] V. K. Pecharsky and K. A. Gschneidner, Jr., Adv. Mater. (Weinheim, Ger.) **13**, 683 (2001).
[20] V. K. Pecharsky and K. A. Gschneidner, Jr., Appl. Phys. Lett. **70**, 3299 (1997).
[21] V. K. Pecharsky and K. A. Gschneidner, Jr., Adv. Cryog. Eng. **43**, 1729 (1998).
[22] A. O. Pecharsky, K. A. Gschneidner, Jr., V. K. Pecharsky, and C. E. Schindler, J. Alloys Compd. **338**, 126 (2002).
[23] L. Morellon, J. Blasco, P. A. Algarabel, and M. R. Ibarra, Phys. Rev. B **62**, 1022 (2000).
[24] C. Magen, L. Morellon, P. A. Algarabel, C. Marquina, and M. R. Ibarra, J. Phys.: Condens. Matter **15**, 2389 (2003).
[25] V. K. Pecharsky, A. P. Holm, K. A. Gschneidner, Jr., and R. Rink, Phys. Rev. Lett. **91**, 197204 (2003).
[26] A. P. Holm, V. K. Pecharsky, K. A. Gschneidner, Jr., R. Rink, and M. Jirmanus, Rev. Sci. Instrum. **75**, 1081 (2004).
[27] C. Magen, Z. Arnold, L. Morellon, Y. Skorokhod, P. A. Algarabel, M. R. Ibarra, and J. Kamarad, Phys. Rev. Lett. **91**, 207202 (2003).
[28] J. B. Sousa, M. E. Braga, F. C. Correia, F. Carpinteiro, L. Morellon, P. A. Algarabel, and R. Ibarra, J. Appl. Phys. **91**, 4457 (2002).
[29] L. Morellon, P. A. Algarabel, C. Magen, and M. R. Ibarra, J. Magn. Magn. Mater. **237**, 119 (2001).
[30] Ya. Mudryk, Y. Lee, T. Vogt, K. A. Gschneidner, Jr., and V. K. Pecharsky, Phys. Rev. B **71**, 174104 (2005).
[31] V. K. Pecharsky, G. D. Samolyuk, V. P. Antropov, A. O. Pecharsky, and K. A. Gschneidner, Jr., J. Solid State Chem. **171**, 57 (2003).
[32] G. D. Samolyuk and V. P. Antropov, J. Appl. Phys. **91**, 8540 (2002).
[33] G. D. Samolyuk and V. P. Antropov, J. Appl. Phys. **97**, 10A310 (2005).
[34] B. N. Harmon and V. N. Antonov, J. Appl. Phys. **91**, 9815 (2002); B. N. Harmon, *ibid.* **93**, 4678 (2003).
[35] H. Tang, V. K. Pecharsky, G. D. Samolyuk, M. Zou, K. A. Gschneidner, Jr., V. P. Antropov, D. L. Schlagel, and T. A. Lograsso, Phys. Rev. Lett. **93**, 237203 (2004).
[36] G. Skorek, J. Deniszczyk, and J. Szade, J. Phys.: Condens. Matter **14**, 7273 (2002).
[37] D. Paudyal, V. K. Pecharsky, K. A. Gschneidner, Jr., and B. N. Harmon, Phys. Rev. B **73**, 144406 (2006).
[38] D. Paudyal, V. K. Pecharsky, K. A. Gschneidner, Jr., and B. N. Harmon, Phys. Rev. B **75**, 094427 (2007).
[39] Materials Preparation Center, Ames Laboratory of US DOE, Ames, IA, USA (www.mpc.ameslab.gov).
[40] Ya. Mudryk, A. P. Holm, K. A. Gschneidner, Jr., and V. K. Pecharsky, Phys. Rev. B **72**, 064442 (2005).
[41] B. Hunter, RIETICA-A visual Rietveld program, International Union of Crystallography Commission on Powder Diffraction Newsletter No. 20 (1998), http://www.rietica.org.
[42] V. I. Anisimov, F. Aryasetiawan, and A. I. Lichtenstein, J. Phys.: Condens. Matter **9**, 767 (1997).
[43] B. N. Harmon, V. P. Antropov, A. I. Lichtenstein, I. V. Solovyev, and V. I. Anisimov, J. Phys. Chem. Solids **56**, 1521 (1995).
[44] O. K. Andersen and O. Jepsen, Phys. Rev. Lett. **53**, 2571 (1984).
[45] D. C. Langreth and M. J. Mehl, Phys. Rev. Lett. **47**, 446 (1981).
[46] D. C. Langreth and M. J. Mehl, Phys. Rev. B **28**, 1809 (1983).
[47] C. D. Hu and D. C. Langreth, Phys. Scr. **32**, 391 (1985).
[48] U. von Barth and L. Hedin, J. Phys. C **5**, 1629 (1972).
[49] J. P. Perdew, Phys. Rev. B **33**, 8822 (1986).
[50] J. P. Perdew and Y. Wang, Phys. Rev. B **33**, R8800 (1986).
[51] E. M. Levin, V. K. Pecharsky, and K. A. Gschneidner, Jr., Phys. Rev. B **62**, R14625 (2000).
[52] K. A. McEwen, in *Handbook on the Physics and Chemistry of Rare Earth*, edited by K. A. Gschneidner, Jr. and L. Eyring (North-Holland, Amsterdam, 1978), Vol. 1, Chap. 6, p. 411.
[53] D. H. Ryan, M. Elouneg-Jamróz, J. van Lierop, Z. Altounian, and H. B. Wang, Phys. Rev. Lett. **90**, 117202 (2003).
[54] Z. Min (private communication).
[55] A. O. Pecharsky, K. A. Gschneidner, Jr., and V. K. Pecharsky, J. Appl. Phys. **93**, 4722 (2003).

[56] E. M. Levin, V. K. Pecharsky, and K. A. Gschneidner, Jr., Phys. Rev. B **60**, 7993 (1999).
[57] W. Choe, G. J. Miller, J. Meyers, S. Chumbley, and A. O. Pecharsky, Chem. Mater. **15**, 1413 (2003).
[58] Y. Imry and M. Wortis, Phys. Rev. B **19**, 3580 (1979).
[59] A. Soibel, E. Zeldov, M. Rappaport, Y. Myasoedov, T. Tamegai, S. Ooi, M. Konczykowski, and V. B. Geshkenbein, Nature (London) **406**, 282 (2000).
[60] M. K. Chattopadhyay, M. A. Manekar, A. O. Pecharsky, V. K. Pecharsky, K. A. Gschneidner, Jr., J. Moore, G. K. Perkins, Y. V. Bugoslavsky, S. B. Roy, P. Chaddah, and L. F. Cohen, Phys. Rev. B **70**, 214421 (2004).
[61] S. Misra and G. J. Miller, J. Solid State Chem. **179**, 2290 (2006).
[62] E. T. Teatum, K. A. Gschneidner, Jr., and J. T. Weber, Los Alamos Scientific Laboratory Report No. LA-4003, 1968 (Clearinghouse for Federal Scientific and technical Information National Bureau of Standards, U.S. Department of Commerce, Springfield, VA).
[63] V. K. Pecharsky and K. A. Gschneidner, Jr., in *Magnetism and Structure in Functional Materials*, edited by A. Planes, L. Mañosa, and A. Saxena (Springer-Verlag, Berlin, 2005), Chap. 11, p. 199.
[64] Y. C. Tseng, D. Haskel, J. C. Lang, S. Sinogeikin, Ya. Mudryk, V. K. Pecharsky, and K. A. Gschneidner, Jr., Phys. Rev. B **76**, 014411 (2007).